Algorithm Theoretical Basis Document

THE BLENDED GLOBAL BIOMASS BURNING EMISSIONS PRODUCT FROM MODIS AND VIIRS Observations (GBBEPx)

VERSION 3.1

Version 3.1

October, 2019

TITLE: THE BLENDED GLOBAL BIOMASS BURNING EMISSIONS PRODUCT FROM MODIS AND VIIRS OBSERVATIONS (GBBEPx)
VERSION 3.1

AUTHORS:

Xiaoyang Zhang (GSCE, South Dakota State University)
Shobha Kondragunta (NOAA/NESDIS/STAR)
Arlindo Da Silva (NASA)
Sarah Lu (IMSG@NOAA/NWS/NCEP)
Hanjun Ding (NOAA/OSPO)
Fangjun Li (GSCE, South Dakota State University)
Yufeng Zhu (MAXIMUS@NOAA/OSPO)

APPROVAL SIGNATURES:

October 8, 2019
Hanjun Ding (OSPO) Date
GBBEPx Product Area Lead

DOCUMENT HISTORY
DOCUMENT REVISION LOG

The Document Revision Log identifies the series of revisions to this document since the baseline release. Please refer to the above page for version number information.

DOCUMENT TITLE: Algorithm Theoretical Basis Document Standards and Guidelines			
DOCUMENT CHANGE HISTORY			
Revision No.	**Date**	**Revision Originator Project Group**	**CCR Approval # and Date**
1.0	N/A	No version 1	N/A
2.0	September 2017		
3.0	September 2019		May 2019
3.1	October 2019	Update to OSPO environment	CCR9849 October 2019

LIST OF CHANGES

Significant alterations made to this document are annotated in the List of Changes table.

DOCUMENT TITLE: The NOAA Blended Polar Geo Biomass Burning Emissions Product (GBBEPx)					
LIST OF CHANGE-AFFECTED PAGES/SECTIONS/APPENDICES					
Version Number	**Date**	**Changed By**	**Page**	**Section**	**Description of Change(s)**
1.0	02/2014				First version in operation
2.0	09/2017				Second version in operation
3.0	08/2019				Third version in operation
3.1	10/2019				Update to OSPO environment

TABLE OF CONTENTS

1. INTRODUCTION

The objective of this document is to provide the Algorithm Theoretical Basis Document (ATBD) of the Blended Global Biomass Burning Emissions Product (GBBEPx V3) from Moderate Resolution Imaging Spectroradiometer (MODIS) and Visible Infrared Imaging Radiometer Suite (VIIRS) (Note that fire detections from geostationary satellites of AHI and ABI are not available). The intended users of the ATBD are end users of the products, Product Area Leads (PALs), and product verification and validation (V&V) teams.

The purpose of the ATBD is to provide a theoretical description (scientific and mathematical) of the algorithm that is used to create a global biomass burning emissions product that meets user requirements.

1.1 Product Overview

Biomass burning releases trace gases [e.g., carbon monoxide (CO), carbon dioxide (CO_2), and methane (CH_4)] and aerosol emissions, which play a significant role in atmospheric chemistry. For example, the emissions from biomass burning account for about 32% of CO and 40% of CO_2 released to the atmosphere globally (Levine, 1996). These emissions and their long-distance transports contribute significantly to the uncertainty in simulating climate change and global warming (Twomey, 1977). They also affect both local and global air quality that has strong impacts on human health and environmental pollution (Seiler and Crutzen, 1980; Phuleria et al., 2005; Sapakota et al., 2005). Currently, the aerosol emitted from biomass burning is one of the major sources of uncertainty in air quality forecasting using models such as the Community Multi-scale Air Quality (CMAQ) (Dennis et al., 1996; Byun and Schere, 2006; Eder and Yu, 2006), and is a critical air pollutant subject to the National Ambient Air Quality Standards (NAAQS) established by the United States (US) Environmental Protection Agency (EPA) (EPA, 2003). Therefore, the availability of information on fires and emissions in near real time for air quality modeling becomes critical.

A large number of research efforts have been devoted to deriving biomass burning emissions using burned area and fuel loading on regional to global scales (e.g., Seiler and Crutzen, 1980; van der Werf, 2006; Wiedinmyer et al., 2006; Zhang et al., 2008; Al-Saadi et al., 2008; Urbanski et al., 2011). The global biomass burning emissions were previously estimated using statistical and inventory data (Seiler and Crutzen, 1980; Hao and Liu, 1994; Andreae and Merlet, 2001). These data are generally incomplete and only available for specific time periods and the results are of high uncertainty. The global biomass burning emissions for specific years include: (1) monthly emissions at a 0.5°×0.5° spatial resolution in 2000 from GLOBSCAR, LPJ-DGVM (the Lund_Potsdam-Jena Global Dynamic Vegetation model), and land cover map (Hoelzemann et al., 2004); (2) monthly 0.5°×0.5° grid emissions in 2000 using burned area from GLOBSCAR and GBA and fuel loading from the terrestrial component of the ISAM (Integrated Science Assessment Model) terrestrial ecosystem mode

(Jain et al., 2006); (3) monthly satellite pixel scale emissions from burned area of GBA-2000 data and global fuel loading maps developed from biomass density data sets for herbaceous and tree-covered land together with global fractional tree and vegetation cover maps (Ito and Penner, 2004); (4) the Global Fire Emissions Database (GFED3.1) at a monthly temporal resolution and a 0.5°x0.5° spatial resolution from 1997-2009 using MODIS active fire data and global biogeochemical modeling (van der Werf et al., 2010); (5) GFED4.0 that is daily and 3-hourly global fire emissions disaggregated from monthly GFED3 using MODIS active fires and GOES WF_ABBA fire observations (Mu et al., 2011; Randerson et al., 2015); (6) the Fire Inventory from NCAR (FINNv1) produced using daily MODIS hotspots from 2005-2010 at a spatial resolution of 1km and fuel loadings assigned to five land cover types (Wiedinmyer et al., 2011); (7) the Wildland Fire Emissions Information System (WFEIS) that calculates fuel consumption and emissions with an open-source version of the Consume model using a tool that provides web access to MODIS burned area and the Monitoring Trends in Burn Severity products, and 1-km fuel maps for the United States (French et al., 2014). These results that were derived from different model inputs vary substantially and the quality of emission estimates is difficult to verify (Li et al. 2019). The uncertainty is mainly from the parameters (burned area, fuel loading, factor of combustion, and factor of emission) used for the estimates of biomass burning emissions.

Fire radiative power (FRP) has recently emerged as an alternative approach to estimate biomass burning emissions. FRP reflects a combination of the fire strength and size and is related to the rate of biomass combustion. Fire radiative energy (FRE) is temporally-integrated FRP, and is related to the total amount of biomass combusted. Thus, it provides a means to directly measure biomass combustion from satellite data (Wooster et al., 2003). Satellites observe fires through the radiant component of the total energy released from fires, providing an instantaneous measurement of fire radiance representing FRP - the rate of FRE release (Kaufman et al., 1998; Wooster et al., 2003; Ichoku et al., 2005). FRP is a proxy for the rate of consumption of biomass and is a function of area being burned, fuel loading, and combustion efficiency. Observed FRP has been successfully used to calculate biomass combusted from wildfires using SEVIRI (Spinning Enhanced Visible and Infrared Imager) radiometer onboard the geostationary Meteosat-8 platform in Africa (Roberts et al., 2005) and MODIS data in both Africa (Ellicott et al., 2009) and globe (Kaiser et al., 2012; Zhang et al., 2012). Quantifying global biomass burning emissions generally rely on fire observations from polar-orbiting satellites. However, their low overpass frequency limits the application of emission estimates for atmospheric and chemical transport models.

NOAA NWS (National Weather Service) NCEP (National Centers for Environmental Prediction) is developing capabilities to provide global aerosol forecasts. This forecast model is called Global Forecast System (GFS) based on NOAA Environmental Modeling System (NEMS), NEMS-GFS, which includes an aerosol model of NASA Goddard Chemistry Aerosol Radiation and Transport Model (GOCART). In addition, NOAA Air Resources Laboratory

(ARL) is conducting air quality forecasting across the United States using the Community Multiscale Air Quality Modeling System (CMAQ). The regional and global models need biomass burning emissions sources (fires) as input. There is a need for timely update of emissions on a daily basis globally. The global biomass burning emissions product, which is derived by blending quick fire emissions data (QFED) from polar-orbiting satellites of Terra and Aqua MODIS and VIIRS fire detections from SNPP and JPSS1 satellites (Note that fire detections from geostationary satellites of AHI and ABI are not available), will meet requirements for the GOCART and CMAQ models. This global operational product is named as GBBEPx V3. It operationally produces daily biomass burning emissions with a one-day latency. The produced species of daily biomass burning emissions with the product output files named as the following:

(1) Daily biomass burning emissions at a grid scale of 0.25°x0.3125°
- GBBEPx_BC.emisions_v003_yyyymmdd.nc – daily emissions of BC with latitude and longitude.
- GBBEPx_CO.emisions_v003_yyyymmdd.nc – daily emissions of CO with latitude and longitude.
- GBBEPx_CO2.emisions_v003_yyyymmdd.nc – daily emissions of CO2 with latitude and longitude.
- GBBEPx_OC.emisions_v003_yyyymmdd.nc – daily emissions of OC with latitude and longitude.
- GBBEPx_PM2.5.emisions_v003_yyyymmdd.nc – daily emissions of PM2.5 with latitude and longitude.
- GBBEPx_So2.emisions_v003_yyyymmdd.nc – daily emissions of SO2 with latitude and longitude.

(2) Daily biomass burning emissions at a grid scale of 0.1°x0.1°
- GBBEPx_all01GRID.emissions_v003_yyyymmdd.nc - Daily emissions at 0.1x0.1 degree grid for CO2, CO, SO2, OC, BC, PM2.5, NOx, NH3, and FRP.

(3) Hourly biomass burning emissions at pixel scales from GBBEP-Geo
- GBBEP_Geo.Hourly_emissions.yyyymmdd.003.nc— hourly latitude, longitude, fire radiative energy (FRE), ecosystem type, dry mass burned, and the emissions of PM2.5, BC, CO, CO2. OC, SO2, and burned area. Note that this file name is kept but fire detections from AHI and ABI are not available.

(4) Fire detections record in the HMS format
- GBBEPx.HMS_MODIS_VIIRS.003.yyyymmdd.txt -- longitude, latitude, date, time, pixel size, satellite, and land cover type.

(5) Quality flag in biomass burning emissions:
- GBBEP_Geo.QA.emissions_v003_yyyymmdd.nc -- Emission quality from geostationary satellites. This file is kept but no fire observations from geostationary satellites.

(6) Spatial pattern of PM2.5 emissions:
- GBBEPx_PM2.5.emissions_v003.yyyymmdd.jpg -- Spatial pattern in Pm2.5 in jpg map

(7) Statistic PM2.5 information at continental scale
- GBBEPx_Regional.Total.PM25_v003_yyyymmdd.txt --- Statistic data in PM2.5

(8) Daily biomass burning emissions at a FV3 C384 grid that are generated using Fortran binary output
- GBBEPx.emis_bc.003.yyyymmdd.FV3.C384Grid.tile1.bin
- GBBEPx.emis_bc.003.yyyymmdd.FV3.C384Grid.tile2.bin
- GBBEPx.emis_bc.003.yyyymmdd.FV3.C384Grid.tile3.bin
- GBBEPx.emis_bc.003.yyyymmdd.FV3.C384Grid.tile4.bin
- GBBEPx.emis_bc.003.yyyymmdd.FV3.C384Grid.tile5.bin
- GBBEPx.emis_bc.003.yyyymmdd.FV3.C384Grid.tile6.bin
- GBBEPx.emis_co.003.yyyymmdd.FV3.C384Grid.tile1.bin
- GBBEPx.emis_co.003.yyyymmdd.FV3.C384Grid.tile2.bin
- GBBEPx.emis_co.003.yyyymmdd.FV3.C384Grid.tile3.bin
- GBBEPx.emis_co.003.yyyymmdd.FV3.C384Grid.tile4.bin
- GBBEPx.emis_co.003.yyyymmdd.FV3.C384Grid.tile5.bin
- GBBEPx.emis_co.003.yyyymmdd.FV3.C384Grid.tile6.bin
- GBBEPx.emis_co2.003.yyyymmdd.FV3.C384Grid.tile1.bin
- GBBEPx.emis_co2.003.yyyymmdd.FV3.C384Grid.tile2.bin
- GBBEPx.emis_co2.003.yyyymmdd.FV3.C384Grid.tile3.bin
- GBBEPx.emis_co2.003.yyyymmdd.FV3.C384Grid.tile4.bin
- GBBEPx.emis_co2.003.yyyymmdd.FV3.C384Grid.tile5.bin
- GBBEPx.emis_co2.003.yyyymmdd.FV3.C384Grid.tile6.bin
- GBBEPx.emis_oc.003.yyyymmdd.FV3.C384Grid.tile1.bin
- GBBEPx.emis_oc.003.yyyymmdd.FV3.C384Grid.tile2.bin
- GBBEPx.emis_oc.003.yyyymmdd.FV3.C384Grid.tile3.bin
- GBBEPx.emis_oc.003.yyyymmdd.FV3.C384Grid.tile4.bin
- GBBEPx.emis_oc.003.yyyymmdd.FV3.C384Grid.tile5.bin
- GBBEPx.emis_oc.003.yyyymmdd.FV3.C384Grid.tile6.bin
- GBBEPx.emis_pm25.003.yyyymmdd.FV3.C384Grid.tile1.bin
- GBBEPx.emis_pm25.003.yyyymmdd.FV3.C384Grid.tile2.bin
- GBBEPx.emis_pm25.003.yyyymmdd.FV3.C384Grid.tile3.bin
- GBBEPx.emis_pm25.003.yyyymmdd.FV3.C384Grid.tile4.bin
- GBBEPx.emis_pm25.003.yyyymmdd.FV3.C384Grid.tile5.bin
- GBBEPx.emis_pm25.003.yyyymmdd.FV3.C384Grid.tile6.bin

- GBBEPx.emis_so2.003.yyyymmdd.FV3.C384Grid.tile1.bin
- GBBEPx.emis_so2.003.yyyymmdd.FV3.C384Grid.tile2.bin
- GBBEPx.emis_so2.003.yyyymmdd.FV3.C384Grid.tile3.bin
- GBBEPx.emis_so2.003.yyyymmdd.FV3.C384Grid.tile4.bin
- GBBEPx.emis_so2.003.yyyymmdd.FV3.C384Grid.tile5.bin
- GBBEPx.emis_so2.003.yyyymmdd.FV3.C384Grid.tile6.bin
- GBBEPx.FRP.003.yyyymmdd.FV3.C384Grid.tile1.bin
- GBBEPx.FRP.003.yyyymmdd.FV3.C384Grid.tile2.bin
- GBBEPx.FRP.003.yyyymmdd.FV3.C384Grid.tile3.bin
- GBBEPx.FRP.003.yyyymmdd.FV3.C384Grid.tile4.bin
- GBBEPx.FRP.003.yyyymmdd.FV3.C384Grid.tile5.bin
- GBBEPx.FRP.003.yyyymmdd.FV3.C384Grid.tile6.bin

1.2 Instrument Characteristics

The GBBEPx V3 product is to calculate daily biomass burning emissions (PM2.5, CO, OC, BC, CO2, and SO2) released from wildfires. Although radiance data from satellite instruments are not directly used, GBBEPx V3 product is produced from satellite-derived fire radiative power (FRP). The GBBEPx V3 algorithm estimates FRP using active fire observations from MODIS and VIIRS (not from geostationary satellites of ABI and AHI) (Tables 1-1). Polar orbiting fire observations are provided by the MODIS instruments on the NASA Terra and Aqua spacecraft and VIIRS onboard Suomi National Polar-orbiting Partnership (SNPP) and Joint Polar Satellite System (JPSS-1) (Table 1-1). The MODIS data provide a nominal spatial resolution of 1 km while VIIRS fire data have a spatial resolution of 750m. Each instrument scans a surface location twice a day in low-middle latitudes. Fire hotspots from MODIS and VIIRS fire detections are retrieved based on various spectral thresholds (Giglio et al., 2016; Csiszar et al., 2016). Basically, the algorithm uses mid-infrared band to identify all potential fires, uses thermal band to eliminate clouds, and uses the difference between brightness temperature in mid-infrared band and thermal band to isolate fires from warm background. The FRP is determined from radiance in fire hotspots. Because FRP detections are frequently obstructed by cloud cover, the product of cloud cover observations is collected to adjust the FRP estimation.

The geostationary satellites except for Meteosat 11 have not been included in the GBBEPx V3 because fire detections from ABI and AHI are not available.

2. ALGORITHM DESCRIPTION

2.1. Processing Outline

Biomass burning is linearly correlated to the total emitted fire radiative energy (FRE) (Wooster, 2003). This is due to the fact that the energy content of dry biomass does not vary considerably across different ecosystems and fuel types (Chapin et al., 2002), and that the actual heat yield in a fire event is slightly influenced by environmental factors including slope, fuel arrangement, and wind speed (Whelan, 1995). The total amount of energy released per unit mass of dry fuel fully burned ranges from 16 to 22 MJ/kg (Lobert and Warnatz, 1993; Whelan, 1995; Trollope et al., 1996; Wooster et al., 2005).

The data processing is outlined in Figures 2-1 and 2-2. Briefly, QFED (version 2) calculates MODIS FRP in individual grid cells for four different biome types, respectively. These biomes are tropical forest, extratropical forest, savanna, and grassland. The fire occurrence in cloud covered pixels is assumed to have the same possibility as that in cloud-free pixels within a grid cell. This process is separated for Terra MODIS and Aqua MODIS data. The coefficient to estimate daily biomass burning emissions from MODIS FRP for four biome types is determined by comparing with GFED (Global Fire Emissions Database) and MODIS aerosol optical depth (AOD).

VIIRS fire emissions are calculated from VIIRS FRP (Figure 2-2). Specifically, VIIRS FRP at a 750m pixel is first obtained from VIIRS NDEAF-L2 fire product. Similar to the processing of MODIS FRP, fire occurrence in cloud covered pixels is also assumed to have the same possibility as that in clear pixels within a grid cell. Then daily FRP flux within a grid cell is calculated using cloud-free observations and the total FRP in a grid cell is the production of FRP flux and grid cell area. The FRP at a continent scale is then linearly associated with QFED. The linear models are used to calculate VIIRS biomass burning emissions. This process is performed for SNPP and JPSS-1 VIIRS separately.

The global biomass burning emissions product (GBBEPx V3) is produced daily by blending VIIRS emissions and QFED in a daily scale.

2.2. Algorithm Input

Fire characteristics are the primary input required for the estimates of biomass burning emissions. These fire data are obtained from fire products derived from polar-orbiting satellites (MODIS and VIIRS) (Tables 1-1). The fire characteristics from MODIS and VIIRS are FRP and cloud mask.

To produce global biomass burning emissions product, a set of static ancillary data is also required (Tables 2-1). For producing QFED, a global 1km MODIS IGBP land cover type is used to stratify land surface into tropical forests, extra-tropical forest, cerrado/woody

savanna, and grassland/cropland. From these land cover types, emissions factors are assigned in the QFED algorithm (Table 2-2).

VIIRS FRP is detected using a very similar approach to MODIS FRP detections (Csiszar et al., 2016), so that these two FRP values are generally comparable. However, these two sensors have different spatial resolutions with different detection capability in small fires (Li et al., 2018). It is assumed that the VIIRS FRP could provide the same fire emissions estimation as QFED at a continental scale. Therefore, the VIIRS FRP is converted to fire emissions using emission coefficients that are derived by comparing daily VIIRS FRP with daily QFED at a continental scale in an entire year (Table 2-4). The coefficients are applied to estimate emissions from both SNPP and JPSS-1.

2.3. Theoretical Description

Biomass burning emissions are conventionally modeled using four fundamental parameters. These parameters are burned area, fuel loading (biomass density), the fraction of biomass combustion, and the factors of emissions for trace gases and aerosols. By integrating these parameters, biomass burning emissions can be estimated using the following formula (Seiler and Crutzen, 1980):

$$E = DM \times F = A \times B \times C \times F \quad (1)$$

where *E* represents emissions from biomass burning (kg); *DM* is the dry fuel mass combusted (kg); *A* is burned area (km^2); *B* is biomass density (kg/km^2); *C* is the fraction of biomass consumed during a fire event; and *F* is the factor of consumed biomass that is released as trace gases and smoke particulates. This simple model has been widely applied to estimate fire emissions in local, regional, and global scales (e.g., Ito and Penner, 2004; Reid et al., 2004; Wiedinmyer et al., 2006; van der Werf et al., 2006; Zhang et al., 2008). The accuracy of the emissions depends strongly on the quality of fuel loading and burned area estimates, which have high uncertainties (e.g., Zhang et al., 2008; van der Werf et al., 2010; French et al., 2011).

Alternatively, Wooster (2003) demonstrated a linear relationship between fuel consumption and total emitted fire radiative energy. This approach avoids the complex estimates of burned area and fuel loadings. Thus, biomass burning emission is linearly linked to fire radiative energy in a simple formula (Wooster, 2003):

$$E = DM \times F = FRE \times \beta \times F = \int FRP \times \beta \times F \quad (2)$$

where *FRP* is fire radiative power (MW), FRE is fire radiative energy (MJ), and β is biomass combustion rate (assumed to be a constant with a value of 0.368±0.015 kg/MJ based on field controlled experiments regardless of the land-surface conditions (Wooster et al., 2005)), F is the emission factor.

2.3.1 Quick Fire Emissions Dataset (QFED)

QFED calculates the flux of biomass burning emissions in each grid cell. Because the details are described by Darmenov and da Silva (2013), the approach is only briefly introduced in the following. According to equation 2, the emission flux (E_{fx}) is described as:

$$E_{fx} = \alpha \times F \times \frac{FRP}{\Delta S} \tag{3}$$

where ΔS is the unit area (Km^2), α is emission coefficient which is similar to combustion factor β but it is defined by comparing with other emissions products.

The FRP density (FRP/ΔS) is calculated from MODIS fire observations. The fire radiative power and the cloud mask are obtained from the MODIS Active Fire product (MOD14 and MYD14) and geolocation is extracted from MODIS Geolocation product (MOD03 and MYD03). By assuming that the FRP density in cloud obscured pixels is equivalent to that in cloud-free pixels, the FRP density in a grid cell is calculated as the following formula:

$$\varphi = \frac{FRP}{\Delta S} = \frac{\varphi_{o,l}\left(A_{o,l} + A_{*,l}\right)}{A_{o,l} + A_{o,w} + A_{*,l}} \tag{4}$$

where φ is FRP density, *o, *, l,* and *w* are used to denote cloud-free, cloud obstruction, land and water, respectively.

After a grid cell is stratified into four biome classes (tropical forest, extratropical forest, savanna, and grassland), the areas of cloud-free, cloud and water pixels are gridded and aggregated for each class of pixels:

$$A(i,j) = \sum_g \sum_p A_p \tag{5}$$

where the summation is done over the pixels from the set of granules *g* that overpassed the grid cell with indexes (i, j). Similarly, the FRPs are gridded and aggregated from the burning pixels:

$$FRP(i,j) = \sum_g \sum_p FRP_p \tag{6}$$

The global gridded QFED fire emissions ($kgm^{-2}s^{-1}$) are calculated using equations from 4 to 7:

$$E_{fx}(i,j) = \frac{\sum_m \alpha_m \sum_b F_{b,s} \times FRP_{m,b}(i,j)}{\sum_m A_m(i,j)} \tag{7}$$

where *m* denotes one of the MODIS fire products, e.g., m = {MOD14, MYD14}, $F_{b,s}$ is emission factors varying with biomes and emission species as defined in the Table 2-2 (Andreae and Merlet, 2001).

Emission coefficient (α) is determined in several steps. The priori value of α is obtained from previous research, which is $a_0 = 1.37 \times 10^{-6}$ kgJ^{-1} reported in Kaiser et al. (2012). Using this coefficient and FRP density, biomass burning emissions are calculated independently

for Terra and Aqua MODIS data. The results were further compared with GFED-v2 using a linear regression form:

$$E_{fx}^{GFED} = \chi_m E_{fx}^{QFED} \quad (8)$$

where the index *m* specifies the MODIS product (MOD14 or MYD14), and the symbol E_{fx} is used to denote the global monthly mean emissions. Finally, the emission factors were corrected as follows:

$$\alpha_m = \chi_m \alpha_0 \quad (9)$$

The comparison of data from 2003-2007 indicates that the factor of $\chi_{MOD14} = 1.38$ for Terra MODIS and $\chi_{MyD14} = 0.47$ for Aqua MODIS. Hence, the emissions coefficients used to calculate the emissions are $\alpha_{MOD14} = 1.89 \times 10^{-6}$ kgJ^{-1} and $\alpha_{MYD14} = 0.644 \times 10^{-6}$ kgJ^{-1}.

The approach was further to define biome-dependent emission strength factors which could deduce fire emissions that improve the agreement between the modeled AOD from NASA Goddard Earth Observing System Model (GEOS-5) and the satellite retrieved AOD. To derive the fire emission strength factors, a multiple regression equation was performed by considering biomass burning and anthropogenic AOD components as independent variables. The contributions from other types of aerosols (e.g., dust, sea-salt, biogenic, volcanic, etc.) were not modified. To fit the AOD from the GEOS-5 to the MODIS AOD observations, a bilinear regression model with two unknown parameters χ_{BB} and χ_{AN} was chosen:

$$\tau* = \tau + (\chi_{BB} - 1)\,\tau_{BB} + (\chi_{AN} - 1)\,\tau_{AN} \quad (10)$$

where τ is the modeled total AOD, and the τ_{BB} and τ_{AN} are the biomass burning and anthropogenic AOD components, respectively. Once the regression parameters of χ_{BB} and χ_{AN} are determined, they are interpreted as the factors by which the strength of the biomass burning and anthropogenic emission needs to be adjusted in order to improve the modeled AOD. A set of strength factors of biomass burning emissions was obtained by analyzing regional mean values of AOD globally. The factors are listed in the Table 2-3.

2.3.2 *Biomass burning emissions estimation from VIIRS observations*

VIIRS fire emissions are converted directly from VIIRS FRP using a set of coefficients. First, VIIRS FRP density is calculated using the same approaches as the calculation of MODIS FRP flux according to equations 3-4 and total FRP in a grid cell is calculated using equations 5-6. Then, the FRP it is assumed that:

$$E_{VIIRS} = \alpha_v FRP_{VIIRS} \quad (11)$$

where E_{VIIRS} is the emissions at a continental scale (kg.s^{-1}) for VIIRS, FRP_{VIIRS} is the total FRP (J.s^{-1}), α_v is a coefficient (kg.J^{-1}).

We assume that fire emissions estimated from VIIRS are the same as QGED (version 2) that is derived from MODIS on Terra and Aqua:

$$E_{VIIRS} = E_{QFED} \tag{12}$$

Based on equations 11 and 12, we can derive the coefficient of α_v:

$$\alpha_v = \frac{E_{QFED}}{FRP_{VIIRS}} \tag{13}$$

The coefficient α_v is derived from SNPP VIIRS FRP and QFED data from April 2016 - March 2017 (Figure 2-3 and Table 2-4). It is thus used to convert VIIRS FRP from both SNPP and JPSS-1 to biomass burning emissions in a grid cell.

2.3.3 Blending QFED and VIIRS emissions

A complete global biomass burning emissions product is generated by blending QFED and VIIRS (on SNPP and JPSS-1). The blended biomass burning emissions (GBBEPx V3) is produced by simply averaging QFED and VIIRS emissions from SNPP and JPSS-1 in a grid cell **(**0.25°x0.315° and 0.1°x0.1°**).** If a product for a given grid cell has no valid value, only the valid values from others are used for generating GBBEPx V3.

2.4 Algorithm Output

The output of global biomass burning emissions (GBBEPx V3) is the blended biomass burning emissions product. It contains a set of daily emissions flux in a grid cell of 0.25°x0.315° and 0.1°x0.1° in netCDF4 files. The emissions in a grid cell of 0.25°x0.315° are further converted to FV3 C384 grids using a nearest neighboring method, where the data are recorded in plain binary files.

Besides a jpg file is produced to visually investigate the spatial distribution of daily PM2.5 emissions and a text file contains the statistics of PM2.5 emissions for quality control purpose.

2.5 Performance Estimates

The GBBEPx V3 algorithm and code have been tested extensively. The test data are the Terra and Aqua MODIS data (MOD03, MYD03, MOD14 and MYD14), and SNPP and JPSS-1 VIIRS data (NDEAF-L2 and GMTCO). Basically, the code has been running routinely in a local machine before official operation.

The fire detections from Terra/Aqua MODIS and SNPP and JPSS-1 VIIRS are the primary inputs, while satellite sensor data are not directly used in biomass burning emissions. However, some fires are not able to be detected because of weak fire radiance, cloud/smoke effects, and satellite instrument saturation. Moreover, false fire detections also happen

because of low radiance contrast between fires and background. Detailed fire detection quality could be found from documents of VIIRS active fire and MODIS fire products.

The primary sources of error in biomass burning emissions are caused by the factors: active fires are not appropriately detected; emission factors obtained from field measurements are uncertain (Andreae and Merlet, 2001); active fires are not observable during cloud cover periods; and daily fire FRP observations are only four times from MODIS and four times from VIIRS.

2.6 Practical Considerations

QFED and VIIRS emissions are performed respectively because the fire detections are totally different. They require different ancillary data (cloud mask and land cover types for QFED and VIIRS emissions) to estimate FRP and corresponding emissions.

The numerical implementation uses Perl scripts to link various parts of calculations, and C programs to calculate pixel based data and to create netCDF files, and IDL to generate jpg images.

In the implement of biomass burning emissions, the algorithm reads fire data as the dynamic input. The fire hotspots vary in each calculation, which results in the change in computing time. For example, a large number of fires appear during fire season while fires are limited during cold and rainy season.

2.7 Validation

Validation of biomass burning emissions is currently impossible because the direct field measurement is very complex. Alternatively, comparison of emission calculation from different estimates could improve our understanding of the GBBEPx V3 quality.

The QFED (before scaled up using AOD) was compared with the commonly used GFED, the FRP based GFAS and the FLAMBE inventories with monthly mean emissions in various regions (Darmenov and da Silva, 2013). The results from 2003-2010 demonstrate that QFED values are distributed within a reasonable range (Figure 2-4).

3. ASSUMPTIONS AND LIMITATIONS

3.1. Performance Assumptions

There are several assumptions in GBBEPx V3 algorithm:

- FRP from polar and geostationary satellites equivalently accurate and reliable.
- Diurnal pattern in FRP from geostationary satellites is generally stable.
- MODIS FRP observed four times a day is acceptable for representing daily FRE.
- MODIS AOD is appropriate to use as a reference to calibrate QFEDv2.
- VIIRS FRP observed four times a day has a good representative of daily emissions.

The major limitations in current GBBEPx V3 are:

- Resolution is very coarse in temporal FRP observations from polar-orbit satellites and in spatial FRP from geostationary satellites
- Combustion factor converting FRE to dry mass combustion is of uncertainties.
- Scaling factors will vary with aerosol models or model parameters
- Fires under forest canopy and clouds are not detectable from satellites.
- Lack of ground truth of biomass burning emissions

3.2. Potential Improvements

The GBBEPx V3 algorithm could be enhanced by fusing polar-orbiting satellite FRP and geostationary satellite FRP directly before estimating biomass burning emissions. Further, FRP from geostationary satellites may have different accuracy from nadir to edge of observations because the fire detection rate may be reduced with view angle increase. Fire detections from ABI and AHI from new generation of geostatianry satellites should be used to replace the observations from current geostationary satellites.

4. REFERENCES

Al-Saadi, J., Soja, A., Pierce, R.B., Szykman, J., Wiedinmyer, C., Emmons, L., Kondragunta, S., Zhang, X., Kittaka, C., Schaack, T., Bowman., K., 2008, Evaluation of Near-Real-Time Biomass Burning Emissions Estimates Constrained by Satellite Active Fire Detections. *Journal of Applied RemoteSensing* , v2, DOI: 10.1117/1.2948785.

Andreae, M.O. and P. Merlet, 2001, Emission of trace gasses and aerosols from biomass burning, *Global Biogeochemical Cycles*, 15(4), p.p. 955−966.

Byun, D.W. and Schere, K.L., 2006, Review of the governing equations, computational algorithms, and other components of the Models-3 Community Multiscale Air Quality (CMAQ) modeling system. *Appled Mechanics Rev*iews, **59**, 51-77.

Campbell, J., Donato, D., Azuma, D., & Law, B. (2007). Pyrogenic carbon emission from a large wildfire in Oregon, United States. Journal of Geophysical Research: Biogeosciences, 112, G04014

Chapin, F.S., Rupp, T.S., Starfield, A.M. et al., 2003, Planning for resilience: modeling change in human-fire interactions in the Alaskan boreal forest, *Frontiers in Ecology and the Environment*, 1, 255–261.

Csiszar, I., Schroeder, W., Giglio, L., Mikles, V., and Tsidulko, M. 2016, The NOAA NDE Active Fire EDR External Users Manual, edited, pp. 1-19.

Darmenov, A., and da Silva, A. 2013, The Quick Fire Emissions Dataset (QFED) - Documentation of versions 2.1, 2.2 and 2.4, In M. J. Suarez (Editor), *Technical Report Series on Global Modeling and Data Assimilation*, Volume 32.

Dennis, R.L., Byun, D.W., Novak, J.H., Galluppi, K.J., Coats, C.J., and Vouk, M.A., 1996, The next generation of integrated aire quality modeling: EPA'S Models-3, *Atmospheric Environment*, *30*, 1925-1938.

Eder, B., and Yu, S. 2006, A performance evaluation of the 2004 release of Models-3 CMAQ, *Atmospheric Environment*, 40, 4811–4824.

Ellicott, E., Vermote, E., Giglio, L., and Roberts, G., 2009, Estimating biomass consumed from fire using MODIS FRE, *Geophysical Research Letters*, 36, L13401, doi:10.1029/2009GL038581.

EPA, 2003, *National Ambient Air Quality Standards (NAAQS)*, Research Triangle Park. NC, USA; http://www.cpa.goviairs/criteria.htntl.

Freeborn, P.H., Wooster, M.J., Roberts, G., 2011, Addressing the spatiotemporal sampling design of MODIS to provide estimates of the fire radiative energy emitted from Africa, *Remote Sensing of Environment*, 115, 475-489.

French, N.H.F., McKenzie, D., Erickson, T., Koziol, B., Billmire, M., Endsley, K.A., Scheinerman, N.K.Y., Jenkins, L., Miller, M.E., Ottmar, R., & Prichard, S. (2014). Modeling Regional-Scale Wildland Fire Emissions with the Wildland Fire Emissions Information System. *Earth Interactions*, 18(16):1-26.

Ghimire, B., Williams, C.A., Collatz, G.J., & Vanderhoof, M. (2012). Fire-induced carbon emissions and regrowth uptake in western U.S. forests: Documenting variation across forest types, fire severity, and climate regions. Journal of Geophysical Research: Biogeosciences, 117, G03036

Giglio, L., Schroeder, W., Csiszar, I., and Tsidulko, M., 2016, Algorithm Theoretical Basis Document For NOAA NDE VIIRS Active Fire, Available: https://www.star.nesdis.noaa.gov/jpss/documents/ATBD/ATBD_NDE_AF_v2.6.pdf, last accessed on 6/2/2017

Hao, W.M., and Liu, M.H. 1994, Spatial and temporal distribution of tropical biomass burning, *Global Biogeochemical Cycles*, *8*(4), 495-504.

Hillger, D., Brummer, R., Grasso, L., Sengupta, M., DeMaria, R., and DeMaria, M., 2009, Production of proxy datasets in support of GOES-R algorithm development, *Proceedings SPIE* 7458, 74580C (2009); doi:10.1117/12.828489

Ichoku, C., and Kaufman, Y.J. 2005, A method to derive smoke emission rates from MODIS fire radiative energy measurements, *IEEE Transactions on Geoscience and Remote Sensing*, 43(11), p.p. 2636-2649.

Ito, A. and Penner, J.E. 2004, Global estimates of biomass burning emissions based on satellite imagery for the year 2000, *Journal of Geophysical Research*, 109(D14S05), doi:10.1029/2003JD004423.

Jain, A.K., Tao, Z., Yang, X., and Gillespie, C., 2006, Estimates of global biomass burning emissions for reactive greenhouse gases (CO, NMHCs, and NOx) and CO2, *Journal Of Geophysical Research*, 111, D06304, doi:10.1029/2005JD006237.

Kaiser, J.W., Heil, A., Andreae, M.O., Benedetti, A., Chubarova, N., Jones, L., Morcrette, J.J., Razinger, M., Schultz, M.G., Suttie, M., and van der Werf, G.R., 2012, Biomass burning emissions estimated with a global fire assimilation system based on observed fire radiative power, *Biogeosciences*, 9, 527-554, doi:10.5194/bg-9-527-2012.

Kaufman, Y.J., Kleidman, R.G., and King, M.D. 1998, SCAR-B fires in the tropics: Properties and their remote sensing from EOS-MODIS, *J. Geophys. Res*., 103, 31,955– 31,969.

Keeley, J.E., & Zedler, P.H. (2009). Large, high-intensity fire events in southern California shrublands: debunking the fine-grain age patch model. Ecological Applications, 19, 69-94

Knapp, E.E., Keeley, J.E., Ballenger, E.A., & Brennan, T.J. (2005). Fuel reduction and coarse woody debris dynamics with early season and late season prescribed fire in a Sierra Nevada mixed conifer forest. Forest Ecology and Management, 208, 383-397

Levine, J.S., 1996, *Biomass Burning and Global Change*, The MIT Press, Cambridge, MA.

Lobert, J.M., and Warnatz, J., 1993, Emissions from the combustion process in vegetation, in Fire in the Environment: *The Ecological, Atmospheric and Climatic Importance of Vegetation Fires*, edited by P. J. Crutzen and J. G. Goldammer, pp. 15– 39, John Wiley, Hoboken, N. J.

Li, F., Zhang, X., Kondragunta, S., Csiszar, I., 2018, Comparison of fire radiative power estimates from VIIRS and MODIS observations. *Journal of Geophysical Research-Atmosphere*, 123(9): 4545-4563.

Li, F., Zhang, X**.**, Roy, D.P., Kondragunta, S. 2019, Estimation of biomass-burning emissions by fusing the fire radiative power retrievals from polar-orbiting and geostationary satellites across the conterminous United States, *Atmospheric Environment*, 211, 274-287.

Mu, M., Randerson, J.T., van der Werf, G.R., Giglio, L., Kasibhatla, P., Morton, D., Collatz, G. J., DeFries, R. S., Hyer, E. J., Prins, E. M., Griffith, D.W.T., Wunch, D., Toon, G.C., Sherlock,V., and Wennberg, P.O., 2011, Daily and 3‐hourly variability in global fire emissions and consequences for atmospheric model predictions of carbon monoxide, *Journal Geophysical Research*, 116, D24303, doi:10.1029/2011JD016245.

Ottmar, R.D., Prichard, S.J., Vihnanek, R.E., & Sandberg, D.V. (2006). Modification and Validation of Fuel Consumption Models for Shrub and Forested lands in the Southwest, Pacific Northwest, Rockies, Midwest, Southeast and Alaska. In: Seattle Washington

Phuleria, H.C., Fine, P.M., Zhu, Y.F., and Sioutas, C., 2005, Air quality impacts of the October 2003 Southern California wildfires, *Journal of Geophysical Research-Atmospheres*, 110(D7), D07S20, doi:10.1029/2004JD004626.

Randerson, J.T., van der Werf, G.R., Giglio, L., Collatz, G.J., and Kasibhatla, P.S., 2015, Global Fire Emissions Database, Version 4, (GFEDv4). ORNL DAAC, Oak Ridge, Tennessee, USA. https://doi.org/10.3334/ORNLDAAC/1293.

Reid, J.S., Prins, E.M., Westphal, D.L., Schmidt, C.C., Richardson, K.A., Christopher, S. A., et al. , 2004, Real-time monitoring of South American smoke particle emissions and

transport using a coupled remote sensing/box-model approach, *Geophysical Research Letter*, 31(L06107), doi:10.1029/2003GL018845.

Roberts, G., Wooster, M.J., Perry, G.L.W., Drake, N., Rebelo, L.M., Dipotso, F., 2005, Retrieval of biomass combustion rates and totals from fire radiative power observations: application to southern Africa using geostationary SEVIRI imagery, *Journal of Geophysical Research*, 110, D21111,, doi:10.1029/2005JD006018.

Sapkota, A., Symons, J.M., Kleissl, J., Wang, L., Parlange, M.B., Ondov, J., Breysse, P. N., Diette, G.B., Eggleston, P.A., and Buckley, T.J., 2005, Impact of the 2002 Canadian forest fires on particulate matter air quality in Baltimore City, *Environmental Science & Technology*, *39* (1), 24-32.

Seiler, W. and Crutzen, P.J., 1980, Estimates of gross and net fluxes of carbon between the biosphere and the atmosphere from biomass burning, *Climatic Change*, *2*, 207-247.

Seiler, W., & Crutzen, P. (1980). Estimates of gross and net fluxes of carbon between the biosphere and the atmosphere from biomass burning. Climatic Change, 2, 207-247

Trollope, W.S.W., Trollope, L.A., Potgieter, A.L.F., and Zambatis, N., 1996, SAFARI-92 characterization of biomass and fire behavior in the small experimental burns in Kruger National Park, *Journal of Geophysical Research,* 101, 23,531– 23,540.

Twomey, S., 1977, The influence of pollution on the shortwave albedo of clouds, *Journal of Atmospheric Science*, *34*, 1149-1152.

Urbanski, S.P., Hao, W.M., and Nordgren, B., 2011, The wildland fire emission inventory: western United States emission estimates and an evaluation of uncertainty, *Atmos. Chem. Phys*., 11, 12973-13000, doi:10.5194/acp-11-12973-2011.

van der Werf, G.R., Randerson, J.T., Giglio, L., Collatz, G.J., Mu, M., Kasibhatla, P.S., Morton, D.C., DeFries, R.S., Jin, Y., and van Leeuwen,T.T., 2010, Global fire emissions and the contribution of deforestation, savanna, forest, agricultural, and peat fires (1997–2009), *ACPD, Vol. 10.,* doi:10.5194/acpd-10-16153-2010

Whelan, R.J., 1995, *The Ecology of Fire*, Cambridge Univ. Press, New York.

Wiedinmyer, C., Quayle, B., Geron, C., Belote, A., McKenzie, D., Zhang, X., O'Neill, S., Wynne, K.K., 2006, Estimating emissions from fires in North America for air quality modeling, *Atmospheric Environment*, 40, p.p.3419–3432.

Wiedinmyer, C., Akagi, S.K., Yokelson, R.J., Emmons, L.K., Al-Saadi, J.A., Orlando, J.J., and Soja, A.J., 2011, The Fire Inventory from NCAR (FINN): a high resolution global model to estimate the emissions from open burning, *Geosci. Model Dev*., 4, 625-641, doi:10.5194/gmd-4-625-2011.

Wooster, M.J., Roberts, G., Perry, G.L.W., and Kaufman, Y.J., 2005, Retrieval of biomass combustion rates and totals from fire radiative power observations: FRP derivation and calibration relationships between biomass consumption and fire radiative energy release, *Journal of Geophysical Research*, 110, D24311, doi:10.1029/2005JD006318.

Wooster, M.J., Zhukov, B., and Oertel, D., 2003, Fire radiative energy for quantitative study of biomass burning: Derivation from the BIRD experimental satellite and comparison to MODIS fire products, *Remote Sensing of Environemt*, 86, 83–107.

Zhang, X. Kondragunta, S., and Quayle, B., 2011. Estimation of biomass burned areas using multiple-satellite-observed active fires. *IEEE Transactions on Geosciences and Remote Sensing,* 49: 4469-4482, 10.1109/TGRS.2011.2149535.

Zhang, X., and Kondragunta, S., 2006, Estimating forest biomass in the USA using generalized allometric model and MODIS land data, *Geographical Research Letter*, *33*, L09402, doi:10.1029/2006GL025879.

Zhang, X., and Kondragunta, S., 2008, Temporal and spatial variability in biomass burned areas across the USA derived from the GOES fire product, *Remote Sensing of Environment*, 112, doi:10.1016/j.rse.2008.02.006.

Zhang, X., Kondragunta, S., Ram, J., Schmidt, C., and Huang, H.C., 2012, Near-real-time global biomass burning emissions product from geostationary satellite constellation, *Journal of Geophysical Research*, 117, D14201, doi:10.1029/2012JD017459.

Zhang, X., Kondragunta, S., Schmidt, C., and Kogan, F., 2008, Near Real Time Monitoring of Biomass Burning Particulate Emissions (PM2.5) across Contiguous United States Using Multiple Satellite Instruments, *Atmospheric Environment,* 42, p.p. 6959-6972.

5. TABLES AND FIGURES

Table 1-1. Inputs of FRP and cloud cover datasets from polar orbit satellites

Satellite/Sensor	Algorithm version	Spatial resolution	Parameters in fire pixels	Temporal resolution
Terra/MODIS : MOD14-Thermal Anomalies/Fire products	Collection 5	1 km	FRP Latitude Longitude Sample and line Number of fire pixels Cloud pixels Clear land pixels	Daily (2 times)
Terra/MODIS: MOD 03 – Geolocation Data Set	Collection 5	1km	Geolocation	Daily (2 times)
Aqua/MODIS: MYD14-Thermal Anomalies/Fire products	Collection 5	1 km	FRP Latitude Longitude Sample Line Number of fire pixels Cloud pixels Clear land pixels	Daily (2 times)
Terra/MODIS: MYD 03 – Geolocation Data Set	Collection 5	1km	Geolocation	Daily (2 times)
VIIRS NDE AF-L2 fire product (AF_v1r1_npp) - Thermal Anomalies/Fire products	Version 1.0	750	FRP Latitude Longitude Sample Line Number of fire pixels	Daily (2 times)

			Cloud pixels Clear land pixels	
Geolocation (GMTCO) product (GMTCO_npp) -- Geolocation Data Set	Version 1.0	750	Geolocation	Daily (2 times)
VIIRS NDE AF-L2 fire product (AF_v1r1_j01) - Thermal Anomalies/Fire products	Version 1.0	750	FRP Latitude Longitude Sample Line Number of fire pixels Cloud pixels Clear land pixels	Daily (2 times)
Geolocation (GMTCO) product (GMTCO_j01) - Geolocation Data Set	Version 1.0	750	Geolocation	Daily (2 times)

Table 2-1. Static input parameters for estimating biomass burning emissions.

Name		Type	Description	Dimension
QFED	MODIS land cover	Input	Pixel data on a 1-km grid	grid (xsize, ysize)
	Emission factors	Input	Table of values for different trace gas species	not applicable
	Scaling factors to AOD	Input	Table of values for different trace gas species	not applicable
GBBEP-Geo	Climatological diurnal pattern of FRP	input	Diurnal FRP variation	not applicable
	Scaling factors for GBBEP-Geo	Input	Table of values	not applicable
	Emission factors	Input	Table of values for different trace gas species	not applicable
VIIRS emissions	Emission factors for VIIRS FRP	Input	Table of values	not applicable

Table 2-2. Emission Factors (g/kg) in computing QFED.

	Tropical Forest	Extra-tropical Forest	Savanna and Grassland
CO2	1580±90	1569±131	1631±95
CO	104±20	107±37	65±20
SO2	0.57±0.23	1.0	0.35±0.16
OC	5.2±1.5	8.6	3.4±1.4
BC	0.66±0.31	0.56±0.19	0.48±0.18
PM2.5	9.1±1.5	13.0±7.0	5.4±1.5

Table 2-4. Biome-dependent emission strength factors for CO, CO_2, OC, BC, SO_2, and $PM_{2.5}$.

	Tropical Forest	Extratropical Forest	Savanna	Grassland
χ_{AN}	1.0	1.0	1.0	1.0
χ_{BB}	2.5	4.5	1.8	1.8

Table 2-5. Coefficients ($kg.J^{-1}$) for VIIRS emissions estimation.

	CO2	CO	PM2.5	OC	BC	SO2
NA	61350	3278	1174	802	61.5	86.9
SA	53189.4	2551	486	298	37.4	31.7
AF	43197.3	2017	360	219	28.9	23.2
EU	69339.4	2925	563	367	42.1	38.6
AS	46529.3	2657	996	677	51.2	73.7
AU	71027	2958	490	311	40.7	32.4

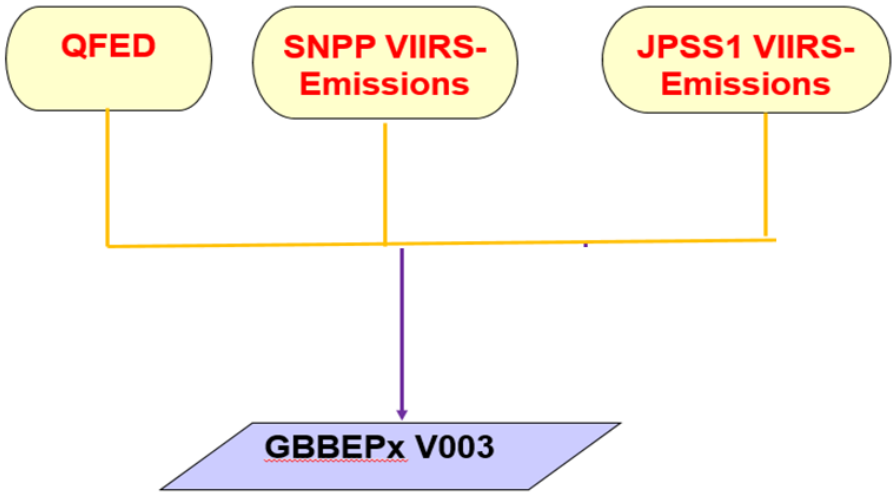

Figure 2-1. Processes of generating the GBBEPx V3 product of biomass burning emissions. QFED is Quick Fire Emission Dataset from MODIS fire data.

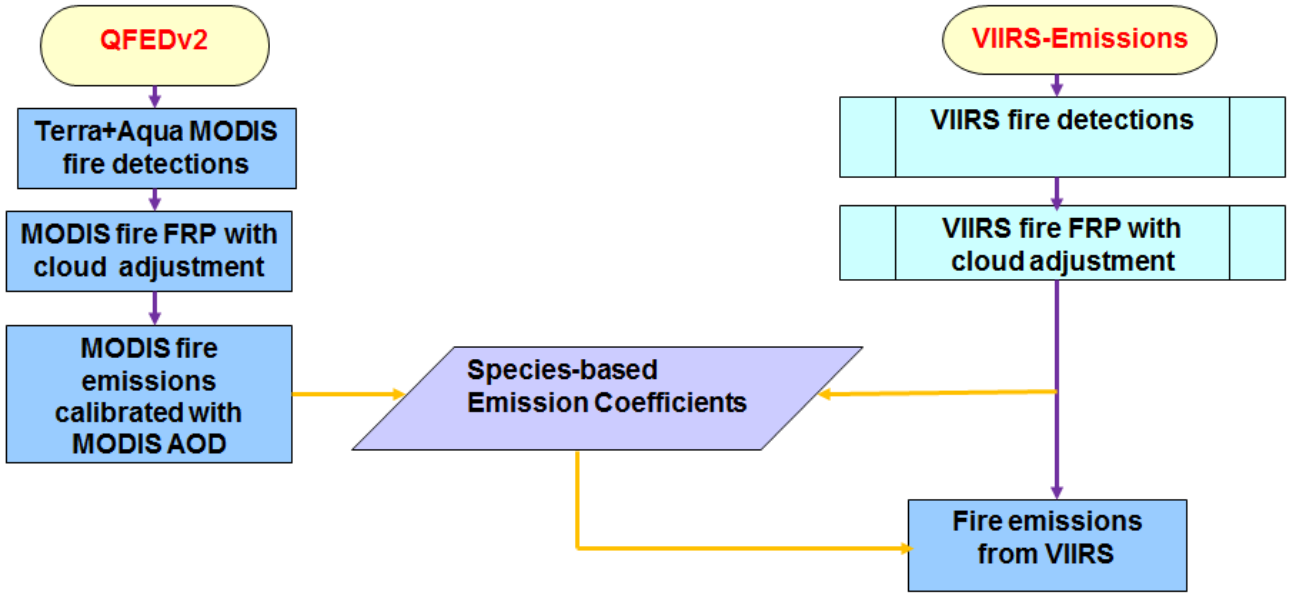

Figure 2-2. Adjusting VIIRS fire emissions using QFED2.

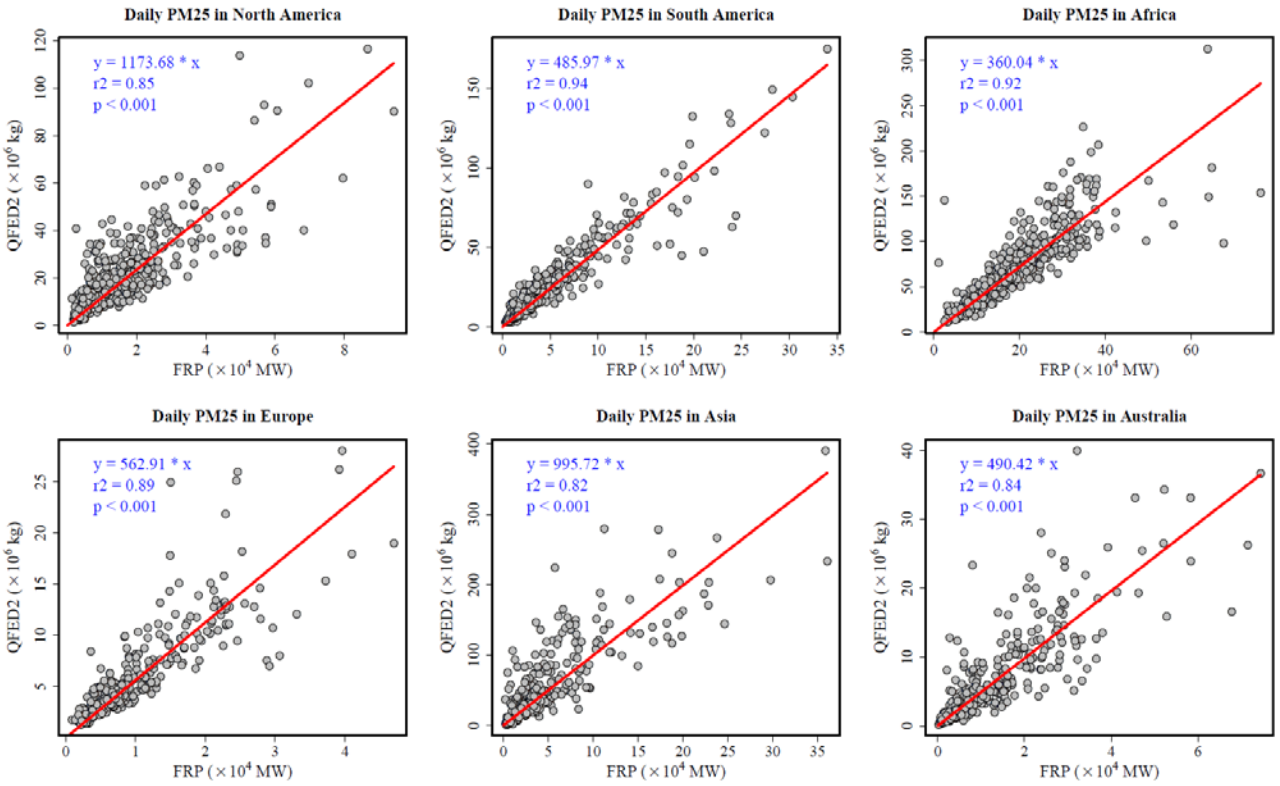

Figure 2-3. Correlation between daily PM2.5 in QFED2 and SNPP VIIRS FRP from April 2016 - March 2017 at each continental scale.

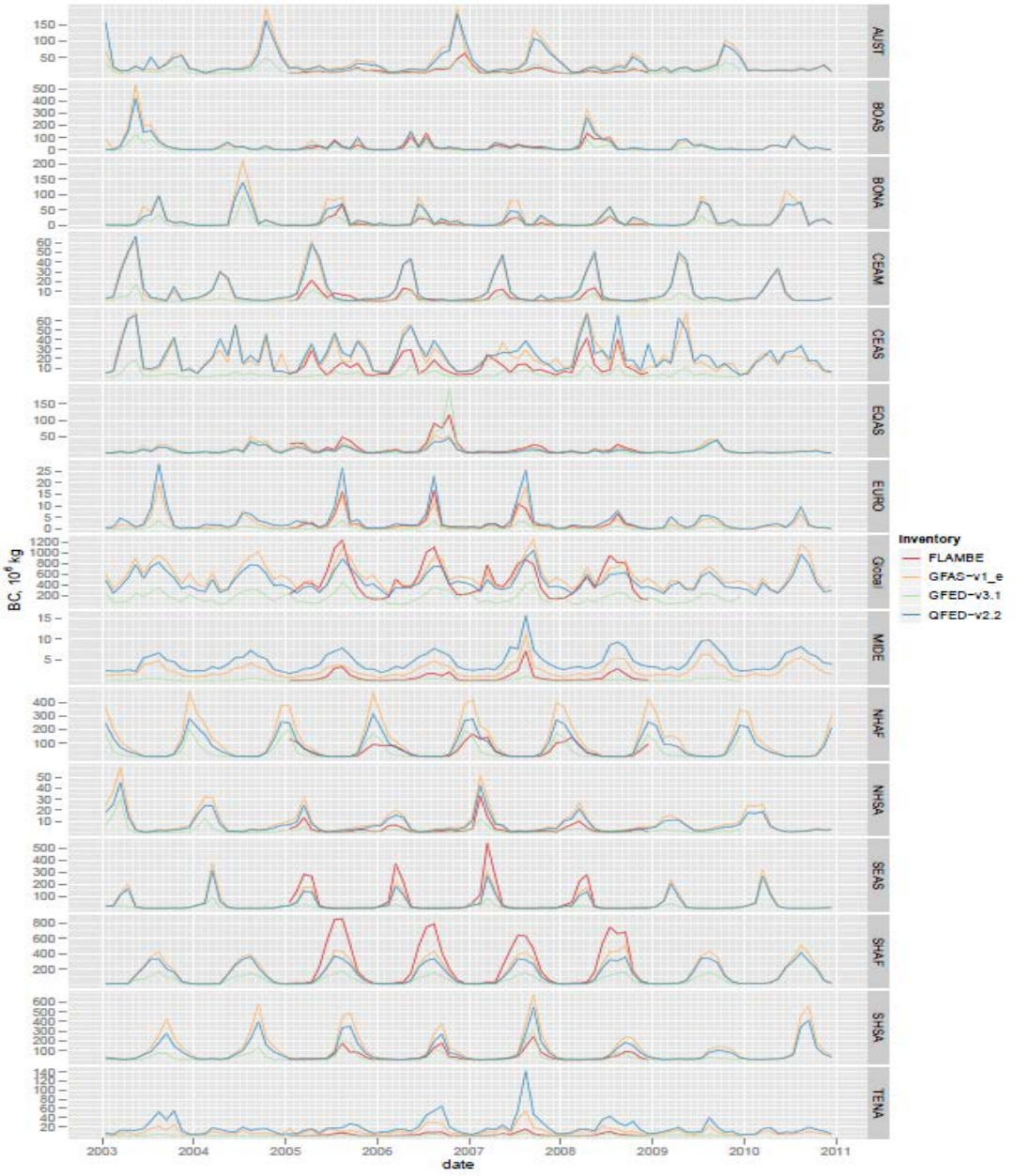

Figure 2-4. Time series of global and regional BC from the QFED, GFED, GFAS, and FLAME inventories (Darmenov and da Silva, 2013). AUST-Australia and New Zealand, BOAS-Boreal Asia, BONA-Boreal North America, CEAM-Central America, CEAS-Central Asia, EURO-Europe, Global-Globe, MIDE-Middle East, NHAF-Northern Hemisphere Africa, NHSA-Northern Hemisphere South America, SEAS-Southeast

Asia, SHAF-Southern Hemisphere Africa, SHSA- Southern Hemisphere South America, TENA-Temperate North America.

ACKNOWLEDGEMENTS

END OF DOCUMENT